(This is a sample cover image for this issue. The actual cover is not yet available at this time.)

Spectrochimica Acta Part A: Molecular and Biomolecular Spectroscopy 109 (2013) 116–124

Contents lists available at SciVerse ScienceDirect

Spectrochimica Acta Part A: Molecular and Biomolecular Spectroscopy

journal homepage: www.elsevier.com/locate/saa

A conformational study of hydroxyflavones by vibrational spectroscopy coupled to DFT calculations

N.F.L. Machado [a], L.A.E. Batista de Carvalho [a], J.C. Otero [b], M.P.M. Marques [a,c,*]

[a] Research Unit "Molecular Physical-Chemistry", University of Coimbra, Rua Larga 3005-535, Coimbra, Portugal
[b] Department of Physical-Chemistry, Faculty of Science, University of Malaga, Campus de Teatinos, 29071 Málaga, Spain
[c] Department of Life Sciences, Faculty of Science and Technology, University of Coimbra, Ap 3046, 3301-401 Coimbra, Portugal

HIGHLIGHTS

- Full vibrational assignment of a series of dietary hydroxyflavones.
- Complete conformational analysis.
- Use of vibrational spectroscopy for establishing reliable structure–activity relationships (SAR's).
- SAR's will allow to understand the health-promoting ability of dietary compounds (phytochemicals).

GRAPHICAL ABSTRACT

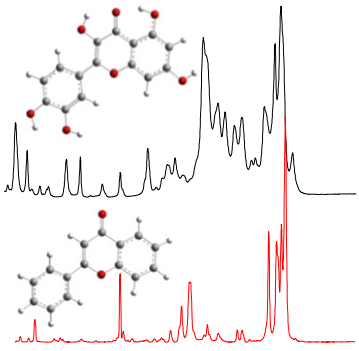

ARTICLE INFO

Article history:
Received 29 October 2012
Received in revised form 9 January 2013
Accepted 11 January 2013
Available online 6 February 2013

Keywords:
Phytochemicals
Chemoprevention
Flavones
Raman
FTIR
DFT calculations

ABSTRACT

The conformational preferences of a series of hydroxyflavones were studied by Raman and FTIR spectroscopies, coupled to Density Functional Theory calculations. Special attention was paid to the effect of hydroxyl substitution, due to its importance on the biological activity of these compounds. Their conformational preferences were found to be determined mainly by the orientation of the hydroxylic groups at C^7 and within the catechol moiety, leading to the occurrence of distinct conformers in the solid state. A complete assignment of the experimental spectra was carried out for these molecules, in the light of their most stable conformers and the corresponding predicted vibrational pattern.

Introduction

Phytochemicals are a class of compounds comprising a wide variety of molecules present in plants, including flavonoids which are known to possess significant health-promoting properties, generally related with their capabilities to act as chain-breaking antioxidants or as radical scavengers [1,2]. In fact, oxidative stress occurs upon disruption of the homeostatic balance between free radical generation and the natural antioxidant defence mechanisms (e.g. by glutathione and regulatory enzymes such as superoxide dismutase, catalase and peroxidases). This is recognised to be directly linked to damage in numerous cell targets (DNA, lipids and proteins) and may therefore lead to severe pathologies such as

* Corresponding author at: Research Unit "Molecular Physical-Chemistry", University of Coimbra, Rua Larga 3005-535, Coimbra, Portugal. Tel./fax: +351 239826541.
E-mail address: pmc@ci.uc.pt (M.P.M. Marques).

1386-1425/$ - see front matter © 2013 Elsevier B.V. All rights reserved.
http://dx.doi.org/10.1016/j.saa.2013.01.038

cardiovascular and neurodegenerative disorders or even cancer. Thus, dietary habits play a key role in the prevention of these diseases since the intake of phytochemicals through the diet, in appropriate amounts, may help to maintain the homeostatic oxidative balance [3].

In the last decade, the beneficial properties of phytochemicals have lead to a vigorous search for novel antioxidants from natural sources, involving the nutritional, pharmacological and medicinal chemistry fields [3–16], with particular emphasis on the prevention of cancer and cardiovascular distress through the consumption of this kind of nutraceuticals in the daily diet [17–20]. Accordingly, special attention has been paid to phenolic acids, anthocyanins, coumarins, tannins and flavonoids (including flavones and isoflavones), the latter being the largest group among phytochemicals [21].

Flavone derivatives, in particular, are known to play an important role in the defence mechanisms against oxidative processes, either from deleterious radical species or from UV radiation. A wide variety of pharmacologically relevant functions is assigned to these compounds [22], from antibacterial, antifungal, antiviral, anti-spasmolytic, estrogen-like, anti-inflammatory and anti-HIV to anticancer [23–31]. This group of compounds contains a common moiety – a chromone skeleton with a phenyl substituent in the pyrone ring (Fig. 1) – which is greatly responsible for their biological role. However, this is also determined by other structural parameters, such as the number and position of the hydroxyl substituent groups, as well as their relative orientation [22,32,33]. In fact, a single variation in one of these factors can induce a considerable change of their biological activity and therefore of their medicinal role. Additionally, this substitution profile also rules the conformational behaviour of the systems, namely their flexibility, the formation of hydrogen bonds – either intra- or intermolecularly – and the preference for planar or skewed relative orientations of the substituent groups. Therefore, the beneficial activity of the flavones and isoflavones under study relies on their structural and conformational behaviour [34–36]. Besides determining biological activity, these strict structure–activity relationships (SAR's) modulate the systemic distribution and bioavailability of the compounds within the cell.

Consequently, it is of the utmost importance to have an accurate conformational knowledge of this kind of phytochemical systems, which can be attained through the combined use of spectroscopic techniques and theoretical approaches. This will lead to a better understanding of their mechanisms of action, and will enable to establish reliable SAR's, crucial for a rational design of effective bioactive compounds based on these natural products. In the present work, the conformational preferences of a series of flavones with different ring substitution patterns were studied by Raman and Fourier transform infrared (FTIR) spectroscopies, coupled to Density Functional Theory (DFT) calculations. The investigated compounds include: – 2-phenylchromone (flavone, FLA), 3,6-dihydroxyflavone (36DH), 5,7-dihydroxyflavone (chrysin, CHRY), 3,3′,4′,7-tetrahydroxyflavone (fisetin, FIS), 3′,4′,5,7-tetrahydroxyflavone (luteolin, LUT) and 3,3′,4′,5,6-pentahydroxyflavone (quercetin, QUER) Fig. 1. The FTIR technique assumes particular importance in the study of this kind of hydroxylated systems, due to its responsiveness in the detection of the vibrational modes related to the OH groups (stretching and bending modes). These will yield relevant information on the conformational preferences of the flavones, closely associated to their biological function. The results thus obtained are related to the free radical scavenging ability of the compounds, which was previously assessed by the authors [37].

Materials and methods

Chemicals

Luteolin (97%) was purchased from Alfa Aesar (Lancashire, United Kingdom). Chrysin (97%), 3,6-dihydroxyflavone (98%), fisetin (⩾99.0%), flavone (⩾98%), and quercetin (⩾98%) were obtained from Sigma–Aldrich Química S.A. (Sintra, Portugal).

FTIR spectroscopy

The FTIR spectra were recorded in a Bruker Optics Vertex 70 FTIR spectrometer, in the 400–4000 cm^{-1} range, in KBr disks (ca. 1% (w/w)). A KBr beamsplitter and a liquid nitrogen cooled Mercury Cadmium Telluride (MCT) detector were used. The spectra were collected for 2 min, with a 2 cm^{-1} resolution. The error in wavenumbers was estimated to be less than 1 cm^{-1}.

Raman spectroscopy

The Raman spectra of FLA, was obtained in a triple monochromator Jobin–Yvon T64000 Raman system (focal distance 0.640 m, aperture f/7.5), equipped with holographic gratings of 1800 grooves mm^{-1}. The premonochromator stage was used in the subtractive mode. The detection system was a liquid nitrogen cooled non-intensified 1024 × 256 pixel (1") Charge Coupled Device (CCD) chip. A 90° geometry between the incident radiation and the collecting system was employed. The entrance slit was set to 200 μm, while the slit between the premonochromator and the spectrograph was set to 400 μm. The spectrum of LUT was acquired in the microconfiguration, using an Olympus BH-2 microscope with a 50× objective. Under the above mentioned conditions, the error in wavenumbers was estimated to be within 1 cm^{-1}.

The 514.5 nm line of an Ar^+ laser (Coherent, model Innova 300-05) was used as the excitation radiation, providing ca. 30 mW at the sample position, except for LUT for which a power of ca. 5 mW was applied (in order to avoid strong fluorescence bands).

Due to their high intrinsic fluorescence, the spectra of 36DH, CHRY, FIS and QUER were recorded in a RFS 100/S Bruker Fourier transform Raman (FT-Raman) spectrometer, with a 180° geometry, equipped with an InGaAs detector. Near-infrared excitation was provided by the 1064 nm line of a Nd:YAG laser (Coherent, model Compass-1064/500N), yielding ca. 250 mW at the sample position, and the resolution was set to 2 cm^{-1}.

The spectra were obtained at room temperature, and the samples were sealed in Kimax glass capillary tubes of 0.8 mm inner diameter, except for microRaman, for which the sample was placed in a glass lamella.

Quantum mechanical calculations

The quantum mechanical calculations were performed using the GAUSSIAN03W program [38] within the Density Functional Theory (DFT) approach, in order to properly account for the electron correlation effects (particularly important in this kind of conjugated systems). The widely employed hybrid method denoted by B3LYP, which includes a mixture of HF and DFT exchange terms and the gradient-corrected correlation functional of Lee et al. [39,40], as proposed and parameterised by Becke [41,42] was used, along with the double-zeta split valence basis set 6-31G** [43]. Molecular geometries were fully optimised by the Berny algorithm, using redundant internal coordinates [44]: The bond lengths to

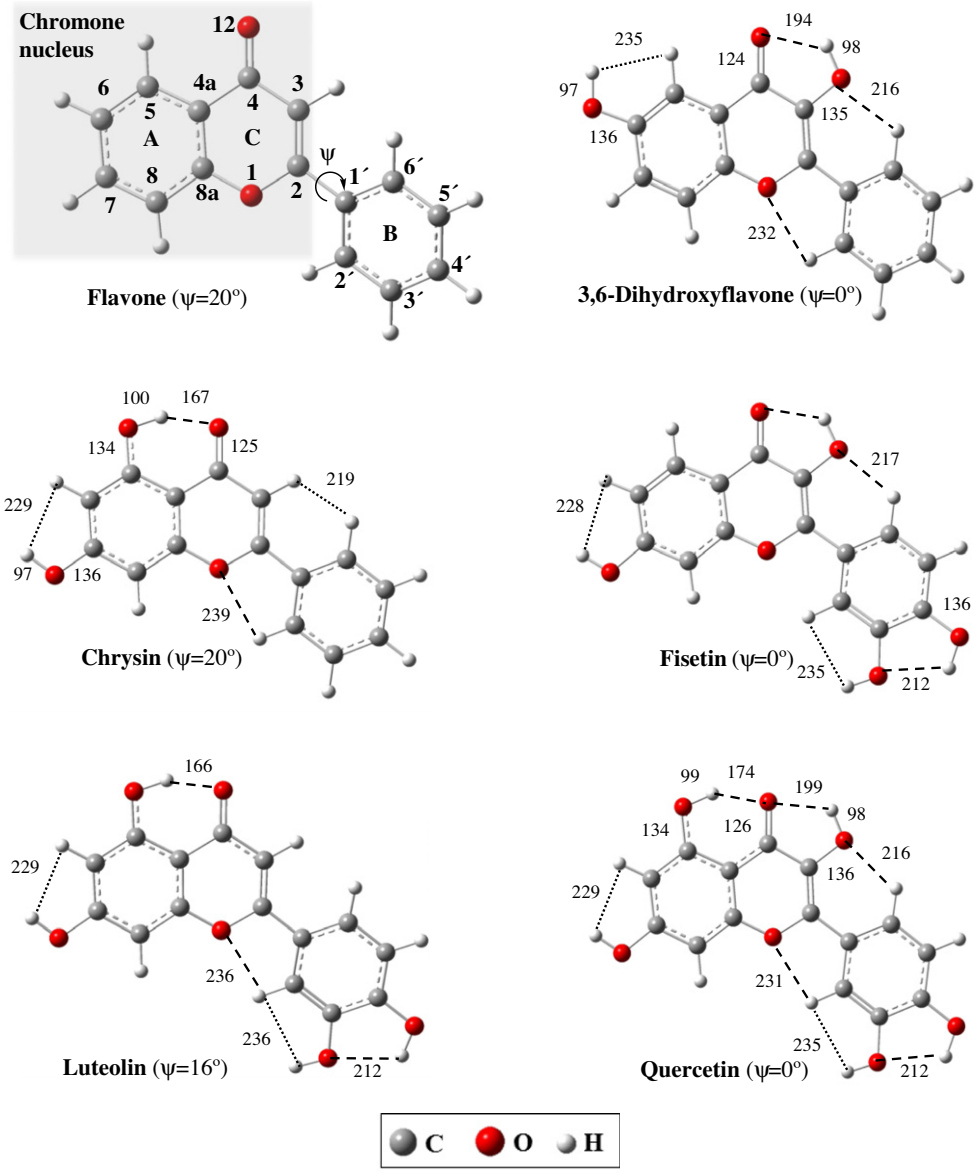

Fig. 1. Calculated (B3LYP/6-31G**) lowest energy geometries for the flavone derivatives presently studied. The atom numbering is included, as well as the possible intramolecular H-bonds (dashed lines) and repulsive interactions (dotted lines). Distances are in pm. ψ represents the ($C^3C^2C^{1'}C^{6'}$) dihedral).

within ca. 0.1 pm and the bond angles to within ca. 0.1°. The final root-mean-square (rms) gradients were always less than 3×10^{-4} hartree bohr^{-1} or hartree radian^{-1}, respectively. No geometrical constraints were imposed on the molecules under study. The relative energies and populations (Boltzman distribution, at 298.15 K) were calculated for all conformers, using the sum of the electronic and zero-point energies (ZPEs).

The harmonic vibrational wavenumbers, as well as the infrared intensities and Raman activities were always obtained at the same level of theory as the geometry optimisation. Given that the widely used Merrick's [45] scale factors do not adequately reproduce the experimental wavenumbers for these highly unsaturated chemical systems, a set of four different factors proposed by the authors for chromone derivatives [46] was used: 1.18 for the low wavenumber region (below 175 cm^{-1}); 1.05 from 175 to 400 cm^{-1}; 0.985 for the interval between 400 and 1500 cm^{-1}; and 0.957 above 3000 cm^{-1}. For the wavenumber range between 1500 and 1850 cm^{-1} Merrick's scale factor of 0.9614 [45] was used.

Results and discussion

Conformational analysis

A full conformational analysis was undertaken for the compounds under study, through DFT calculations. Table 1 summarises the most significant dihedral angles defining the respective most stable conformers.

The conformational behaviour of these compounds is determined by the following structural characteristics:

(A) The presence of a hydroxyl group at position 5 ((O^5H), Fig. 1, which is known to form a strong intramolecular hydrogen bond (H-bond) with the neighbouring carbonyl of the pyrone ring. This close contact yields a six-membered intramolecular ring (Fig. 1) responsible for an enhanced electronic delocalisation that stabilises the molecular structure. This interaction has been extensively studied spectroscopically, being recognised to be stronger than the H-bond between (O^3H) and the ketonic oxygen [47], which gives rise to a five-membered ring instead. For CHRY, for instance,

Table 1
Most stable conformers calculated for the substituted flavones under study.

Compound	Conformational description (dihedral values)[c]							
ΔE[a]	pop.[b] (%)	Ψ	C^2C^3OH	$C6C^5OH$	C^8C^7OH	C^7C^6OH	$C^{2'}C^{3'}OH$	$C^{3'}C^{4'}OH$
FLA								
0.00	100.0	20.3	–	–	–	–	–	–
36DH					–			
0.00	85.8	0.0	180.0	–	–	180.0	–	–
4.47	14.2	0.0	180.0	–	–	0.0	–	–
CHRY					–			
0.00	72.5	19.9	–	−179.9	179.9	–	–	–
2.40	27.5	20.5	–	−179.9	0.1	–	–	–
FIS								
0.00	32.5	0.0	180.0	–	180.0	–	0.0	0.0
0.72	24.3	0.0	180.0	–	0.0	–	180.0	180.0
0.73	24.2	0.0	180.0	–	0.0	–	0.0	0.0
1.32	19.0	0.0	180.0	–	180.0	–	180.0	180.0
LUT								
0.00	55.8	15.8	–	−179.9	179.9	–	−0.7	−0.1
2.56	19.9	18.8	–	0.2	180.0	–	179.8	179.6
3.19	15.4	17.5	–	−179.9	0.3	–	0.1	0.1
4.55	8.9	19.0	–	−179.8	0.0	–	179.6	179.5
QUER								
0.00	42.9	0.0	180.0	180.0	180.0	–	0.0	0.0
1.80	22.2	0.0	180.0	180.0	180.0	–	180.0	180.0
2.39	17.5	0.0	180.0	180.0	0.0	–	0.0	0.0
2.88	14.4	0.0	180.0	180.0	0.0	–	180.0	180.0

[a] Energy differences in kJ mol^{-1} calculated at the B3LYP/6-31G** level.
[b] Boltzmann distribution, calculated at room temperature using the B3LYP/6-31G** electronic energy corrected by the zero-point vibrational value (obtained at the same level of theory).
[c] In degrees. The atoms are labelled according to Fig. 1.

an energy difference of ca. 67.5 kJ mol^{-1} was found between the equilibrium structure and the most stable conformation not comprising this ($O^5H\cdots O$) H-bond. The breakdown of this intramolecular close contact is highly unfavoured in these systems, except in compounds displaying both (O^3H) and (O^5H) groups (such as QUER, Fig. 1) which present a quite different behaviour.

(B) In those molecules containing a catechol moiety, the two hydroxyl groups located at the B-ring (FIS, LUT and QUER, Fig. 1) tend to adopt the same orientation relative to the carbonyl(s): either syn (parallel) or anti (anti-parallel), due to a weak H-bond between both adjacent hydroxylic groups (Fig. 1). The syn conformation is unfavoured relative to the anti one (Table 1). In fact, the former was found to be favoured for all the compounds presently studied, as a result of a more efficient electronic delocalisation.

Among the catechol-like molecules displaying a C^7–OH moiety, the hydroxylic substitution from C^3 to C^5 (FIS to LUT, Fig. 1) leads to dramatic structural changes. In QUER, comprising both C^3 and C^5 hydroxyl groups, a hydrogen close contact may be established between the carbonyl oxygen and the two adjacent hydroxyl H atoms (Fig. 1). This bifurcated H-bond can be regarded as a highly delocalised electronic system and is present in the most stable conformations of this molecule. The breakdown of this interaction in either (O^3H) or (O^5H) is unfavoured by ca. 40 kJ mol^{-1}, respectively, while simultaneous disruption of both H-bonds corresponds to an energy increase of 102 kJ mol^{-1}.

(C) Flavonols have a hydroxyl group in position 3 of the chromone skeleton (36DH, FIS and QUER, Fig. 1) which forms a H-bond with the carbonyl located at C-ring, giving rise to an extra five-membered ring (Fig. 1). This intramolecular close contact is responsible for the stabilisation of the system by electronic delocalisation throughout the molecule. An opposite orientation of the (O^3H) group, in turn, destabilises the system up to 40 kJ mol^{-1} due to steric hindrance effects and to a less efficient electronic delocalisation, leading to a non-planar B-ring.

(D) Regarding planarity, all conformers found for 36DH, FIS and QUER (flavonols) are planar (Table 1), while for FLA, CHRY, LUT (flavones) are non-planar with dihedral angles ψ (($C^3C^2C^{1\prime}C^{6\prime}$), Fig. 1) ranging from 20.3° (FLA) to 15.8° (LUT, Table 1). When the catechol moiety is present, it was found to be coplanar with the rest of the molecule in the case of the flavonols, while it assumes a non-planar structure for the remaining flavones.

The optimised DFT geometries predicted for the isolated molecules under study were compared to the X-ray crystallographic data found in the literature for similar systems: 3-hydroxyflavone (3HF) [48], 5-hydroxyflavone (5HF) [49] and the dihydrated form of QUER [50]. A fairly good agreement was found, the chromone core moiety being essentially planar in all cases. 3HF, an analogous of 36DH, deviates from planarity in the solid state, probably due to both intra- and intermolecular H-bond interactions (ψ = 5.5°), while a planar equilibrium geometry was presently calculated for 36DH (Table 1). Furthermore, the intramolecular H-bond associated to the (O^3H) group seems to be involved in the complex structure of the solid, being responsible for the difference between the calculated $H\cdots O$ distance for 36DH (194 pm) and the experimental value reported for 3HF (220 pm). The H-bond involving the (O^5H) moiety in CHRY yields a calculated distance of 167 pm, close to the experimental value obtained for 5HF in the condensed phase (168 pm) [49]. Finally, the deviation from planarity previously observed for 5HF (ψ = 5.8°) is quite smaller than the one presently predicted for the molecules comprising an (O^5H) group (ψ = 19.9°, Table 1).

In the case of bonded atoms, the agreement between experimental and calculated distances was found to be very good (Table 2). As an example, the C^5–O distance in CHRY is predicted as 133.6 pm, close to the crystallographic value of 135.8 pm obtained for 5HF [49]. In the case of 36DH a distance of 135.3 pm was calculated for the C^3–O bond, in accordance with the experimental value of 135.7 pm reported for 3HF in the solid state [48].

Spectral assignment

A full spectral assignment was performed for these systems, in the light of their predicted conformational preferences (although these were obtained for the isolated molecule) (Tables S1 and S2). Despite the considerable amount of work reported for these systems both by Raman and SERS techniques [51–54], a complete

Table 2
Comparison between X-ray crystallographic structures and the presently calculated ones.

Structural parameter[a]	Solid[b]			Calculated[c]					
	3HF	5HF	QUER	FLA	36DH	CHRY	FIS	LUT	QUER
$C4{=}O^{12}$	123.2	125.3	126.9	123.1	124.4	125.3	124.4	125.4	126.2
C^3O	135.3	–	135.8	–	135.3	–	135.4	–	135.6
C^5O	–	135.8	135.2	–	–	133.6	–	133.6	134.0
$O^3H\cdots O{=}C$	220	–	–	–	194.0	–	194.0	–	198.6
$O^5H\cdots O{=}C$	–	168	–	–	–	166.7	–	166.2	174.1
ψ (°)	5.5	5.8	6.7	20.3	0.0	19.9	0.0	15.8	0.0

[a] Distances in pm; ψ values in degrees. The atoms are labelled according to Fig. 1.
[b] Values obtained from X-ray crystallography [48–50].
[c] Calculated at the B3LYP/6-31G** level, for the lowest energy conformations.

and accurate assignment has not yet been achieved. Furthermore, FTIR has a huge potential for the study of this kind of polyhydroxylated compounds [47,55–57]. The present work intends to attain a thorough vibrational analysis (Raman and FTIR) of these chromone derivatives, concomitantly studied by theoretical methods. The main spectral features that characterise these flavones are therefore described and compared:

(A) In the high wavenumber region, the ν(CH) modes give rise to the most intense (quite sharp) bands in the Raman spectra, between 3000 and 3100 cm^{-1} (Fig. 2). In infrared, in turn, these modes usually yield weak features, often partially overruled by the broad, very intense, ν(OH) bands (with the exception of flavone, that contains no hydroxylic groups) (Fig. 3). The assignment of such bands is not a straightforward task in these systems, since they are very sensitive to the chemical environment: in the case of FLA, for instance, the most intense bands within this region (ca. 3060 and 3070 cm^{-1}) are due to modes from either rings A or B (Fig. 2, Table S1). An exception to this behaviour is found for the (C^3H) oscillator, which is in a somewhat different environment and displays a slight increase of its stretching wavenumber (3107 cm^{-1} in FTIR, Table S1). Furthermore, the presence of different substituents in the series of compounds investigated alters the corresponding electronic distribution, causing marked changes in their vibrational profile, namely regarding the ν(CH) oscillator (Tables S1 and S2).

The ν(OH) modes, also comprised in this high wavenumber spectral interval, contain important information on the conformation of the hydroxyl groups in the molecule, as well as on their involvement in hydrogen close contacts. CHRY is a good example, as the intense and extremely broad band detected between 2500 and 3200 cm^{-1} is due to the strong intramolecular interaction involving the (O^5H) group, this feature being characteristic of 5-hydroxylated chromones [56,57]. LUT presents a similar behaviour, yielding this very broad signal in the FTIR spectrum (Fig. 3). Meanwhile, for QUER a distinct infrared band around 3290 cm^{-1} is to be found, ascribed to the stretching modes of the H-bonded (O^3H) and (O^5H) hydroxyl moieties, while a new Raman band occurs at 3321 cm^{-1}, assigned to $\nu(O^3H)$ (Table S2). Regarding the (O^7H) group, it is probably involved in strong intermolecular H-bond interactions in CHRY, leading to a decrease of the corresponding stretching vibration that shifts to a region where it is masked by the strong $\nu(O^5H)$ signal. Although this mode has been tentatively assigned by other authors to the weak feature at 3010 cm^{-1} [58], the number of bands below 3050 cm^{-1} due to overtones/combination modes, coupled to the high intensity of the $\nu(O^5H)$ feature, render this assignment quite difficult. As to the flavones possessing a catechol group, the $\nu(O^7H)$ band seems to be merged with the strong feature between 3350 and 3400 cm^{-1}, also comprising the catechol's ν(OH) vibrations (Table S2).

The features related to the ν(OH) modes are also clearly visible in the Raman spectra. For 36DH, for instance, the sharp band at 3330 cm^{-1}, assigned to $\nu(O^6H)$, and the very strong broad signal at about 3190 cm^{-1}, corresponding to $\nu(O^3H)$, are detected both in Raman and FTIR (Table S1 and Figs. 2 and 3). For FIS, apart from the two strong bands around 3520 and 3550 cm^{-1} due to hydration (Fig. 3), two intense features are observed: at 3253 cm^{-1}, due to the H-bonded (O^3H) group (also visible by both techniques), and at 3352 cm^{-1}, originated by the stretching of the (O^7H) group, while for QUER the $\nu(O^3H)$ mode is active only in Raman thanks to its proximity to the $\nu(O^5H)$ vibration.

The $\nu(O^3H)$ and $\nu(O^5H)$ experimental wavenumbers obtained for QUER are in good agreement with the bifurcated H-bonding profile predicted for this molecule (previously discussed), the $\nu(O^3H)$ mode being detected at a higher wavenumber than for the other flavonols (Tables S1 and S2). Also, $\nu(O^5H)$ gives rise to a relatively sharper band (at higher wavenumber) than the one usually detected between 2500 and 3200 cm^{-1} (very broad) for the other compounds (Figs. 2 and 3). This behaviour reflects the simultaneous formation of two weaker H-bonds sharing the charge of the carbonyl group, instead of one, stronger, intramolecular hydrogen close contact.

(B) In the spectral interval between 1550 and 1750 cm^{-1}, the wavenumber deviations of the carbonyl stretching mode reflect the nature of the interactions in which this group is involved, therefore providing important information on the hydrogen bonding pattern in this kind of compounds. However, the $\nu(C^4{=}O^{12})$ modes appear in the same region as $\nu(C^2C^3)$ and the deformations of both the aromatic ring and the hydroxylic groups. In the case of the (O^5H) substituted flavones (CHRY, LUT and QUER), the strong coupling between ν(C=O) and aromatic ring deformations is due to the presence of the 6-membered ring formed upon $(C{=})O\cdots H(O^5)$ intramolecular bonding (Fig. 1, Tables S1 and S2).

For FLA, the ν(C=O) mode gives rise to a strong band detectable both in Raman and FTIR, at 1633 and 1646 cm^{-1} respectively (Fig. S1, Table S1), in good accordance with previous reported studies [54]. Additionally, the ν(C=O) experimental values observed for 36DH and CHRY agree well with the predicted ones (Table S1), and the wavenumber difference detected for these compounds is similar to that calculated between 5HF and 3HF, which was interpreted in the light of the distinct nature of the two intramolecular H-bonds [47]. A similar pattern between LUT and QUER can be observed, mainly by infrared, where the carbonyl stretching modes are quite strong (Fig. S1), two intense broad bands being detected at 1656 and 1612 cm^{-1} for LUT, and at 1662 and 1615 cm^{-1} for QUER, both corresponding to vibrations with a large ν(C=O) component. The band at higher wavenumber in the QUER spectrum is significantly broadened, reflecting the bifurcated H-bonding profile within the molecule, as well as the presence of a Fermi Resonance (FR) involving the strong ν(CO) band and overtones or combinations of the signals between 700 and 1000 cm^{-1} (often detected in flavones [57]).

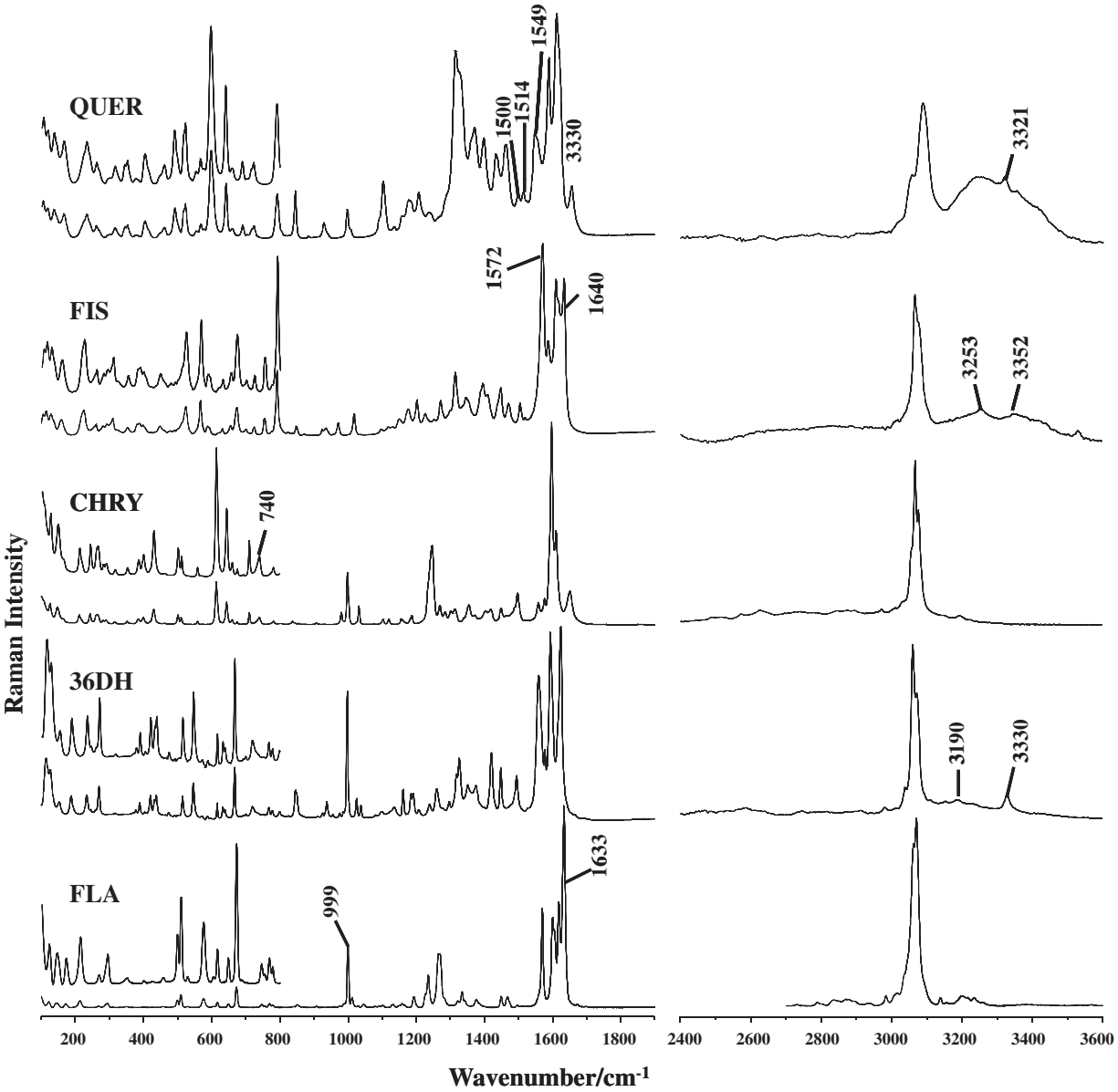

Fig. 2. Experimental Raman spectra (100–1900 and 2400–3600 cm^{-1}) for the presently studied flavones.

FIS presents a completely distinct FTIR and Raman pattern as compared to LUT and QUER, the carbonyl stretching mode being found at a lower wavenumber – 1634 and 1630 cm^{-1} in Raman and FTIR, respectively (Table S2, Fig. S1). Instead of the two broad infrared bands found for LUT and QUER, two sharper, superimposed features were observed, a stronger one at 1607 cm^{-1} and another at 1630 cm^{-1}. A third band is still detected, at 1570 cm^{-1} in FTIR and at 1572 cm^{-1} in Raman (the most intense within this region, Table S2). In fact, within this spectral interval FIS presents the highest similarity with 36DH, also displaying the carbonyl group exclusively bonded to the hydroxyl at O^3.

(C) The hydroxylated flavones display vibrational features associated to δ(OH) modes mixed with ν(C=O), ν(CC) and aromatic ring deformations, in the interval between 1550 and 1000 cm^{-1}. These signals can yield reliable information on the relative orientation of the hydroxylic groups.

The simplest hydroxyl-substituted molecules are 36DH and CHRY, both comprising intramolecular H-bonds. For the former, the strongest FTIR band occurs at 1497 cm^{-1}, while for the latter two intense signals appear at 1500 and 1449 cm^{-1} (Fig. S1). Between these, a series of superimposed features is detected for CHRY (Fig. S1), apart from two strong infrared bands at 1354 and 1169 cm^{-1}, probably related to the presence of distinct (O^7H) orientations within the molecule (Tables 1 and S1).

The systems containing a catechol group (FIS, LUT, and QUER) display a characteristic set of strong infrared bands from 1000 to 1500 cm^{-1} (Fig. 3), which are quite narrow for FIS and broader for the (O^5H) substituted flavones LUT and QUER (Fig. 3). In FIS, several shoulders and superimposed bands are to be found in the FTIR spectrum (e.g. from 1500 to 1550 cm^{-1}), as opposed to the Raman (Fig. S1). This may reflect the presence of two distinct conformations, in agreement with the small calculated energy difference between fisetin's conformers 1 and 2 (0.72 kJ mol^{-1}, Table 1). Additionally, the spectra presently obtained correspond to the hydrated (commercial) compound, which may lead to changes in its conformational preferences relative to the anhydrous molecule.

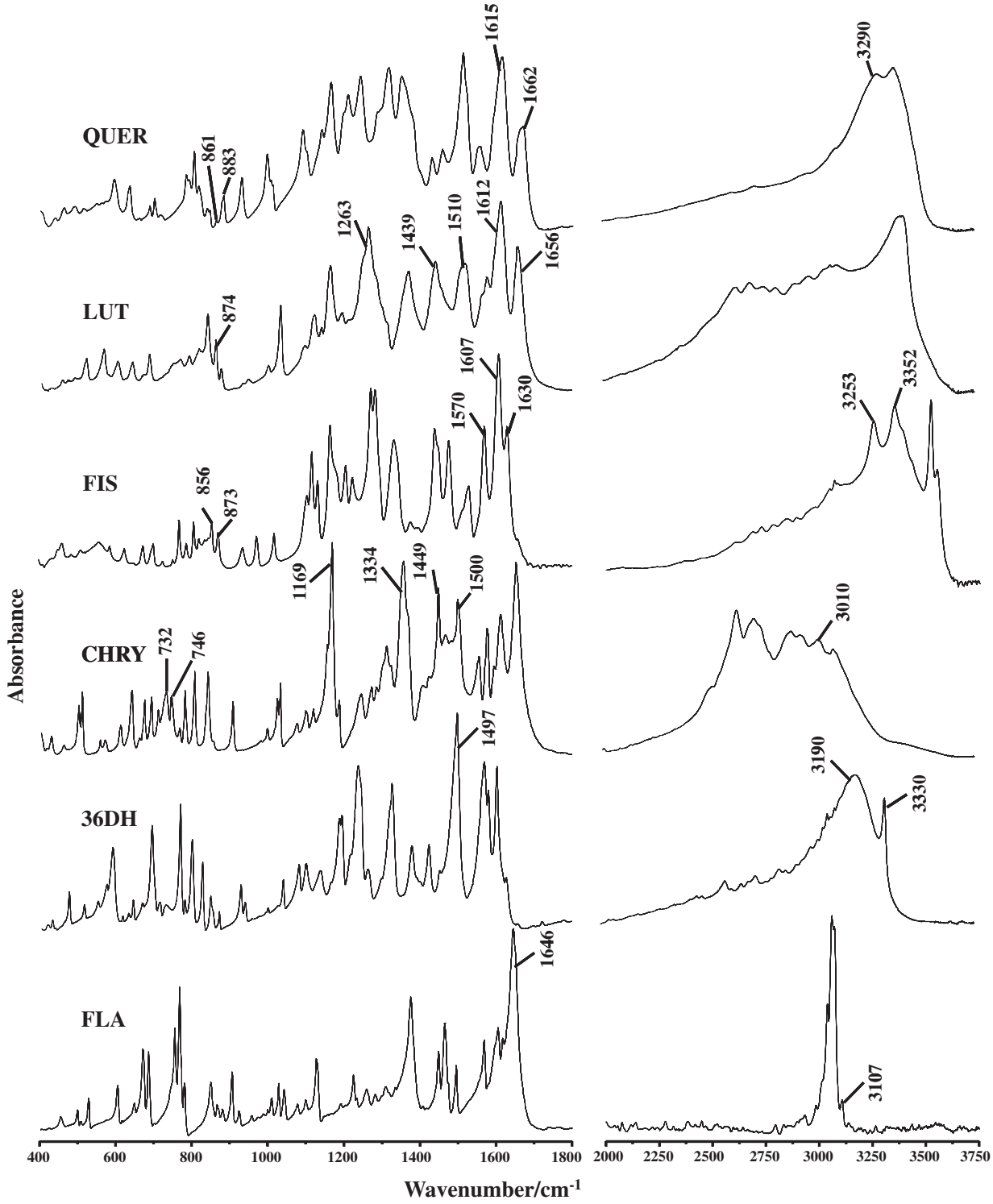

Fig. 3. Experimental FTIR spectra (400–1800 and 2000–3750 cm^{-1}) for the presently studied flavones.

Comparing FIS to the (O^5H) substituted compounds LUT and QUER, the first obvious observation is the presence of ring vibrational modes (8a deformation) at wavenumbers as low as 1549 cm^{-1} in the latter (Table S2, Fig. S1). Furthermore the strongest infrared band for QUER, displaying two shoulders, is centred at ca. 1500 cm^{-1}, while two weak Raman features are found in this wavenumber interval (1500–1514 cm^{-1}, Figs. 2 and S1). Similarly, for LUT a rounded shaped infrared signal around 1510 cm^{-1} (Fig. S1) is detected. This behaviour (and the strong intensity of this band) evidences the presence of conformer 3 in both compounds, the (O^7H) group displaying either a syn or an anti conformation relative to the carbonyl group (Tables 1 and S2). Moreover, LUT displays infrared signals ascribed to the catechol group at 1439 cm^{-1} (with a shoulder to high wavenumber) (Fig. S1), and at 1263 cm^{-1} (the second strongest band in the spectrum), their intensity and width being justified by the presence of distinct orientations of the catechol hydroxylic groups (Tables 1 and S2).

(D) Below 1000 cm^{-1}, the out-of-plane modes – either deformations of the aromatic rings or out-of-plane bendings of the (CH) and (OH) groups – give rise to strong infrared bands, while the corresponding Raman features are generally undetectable, the in-plane modes tending to be more Raman active than the out-of-plane ones.

Besides the band at 999 cm^{-1}, the vibrational spectra of FLA comprises weak Raman signals, in contrast to the large number of strong bands detected in FTIR (essentially assigned to out-of-plane-modes, Table S1 and Figs. 2 and 3). A similar behaviour is observed for CHRY and 36DH, although the Raman features for the latter present a rather higher intensity (Fig. 2).

Within this region, CHRY displays two typical broad FTIR bands, at 746 and 732 cm^{-1} (Fig. 3), while a weak broad signal is found in Raman at ca. 740 cm^{-1} (Fig. 2). The infrared features are due to both in-plane and out-of-plane modes associated to the six-membered intramolecular ring (Table S1), which is responsible for the significant band broadening.

For the catechol-containing compounds, useful information can be obtained from this spectral region. From the set of infrared bands between 860 and 890 cm^{-1}, for instance, those at 873 and 883 cm^{-1} in FIS and QUER (respectively, Fig. 3) are due to an out-of-plane CH bending mode from the catechol group in conformer 2, while the corresponding bands from conformer 1 are found at 856 and 861 cm^{-1} (Table S2). Meanwhile, LUT presents a similar FTIR pattern, although assignment of the 874 cm^{-1} signal to conformer 2 (calculated mode at 886 cm^{-1}) is dubious, since there is a predicted wavenumber at 859 cm^{-1} for conformer 1 (Tables 1 and S2). Also relevant is the set of superimposed infrared bands observed between 750 and 850 cm^{-1} for LUT, FIS and QUER (Fig. 2), tentatively explained by the presence of distinct conformations for these compounds.

Conclusions

A conformational analysis of a series of hydroxylated flavones was carried out, by optical vibrational spectroscopy coupled to theoretical approaches. The DFT calculations allowed to assess the conformational preferences of the compounds, strongly dependent on their intramolecular H-bonding motif.

The compounds under study display two distinct intramolecular interactions, leading to the formation of either 6- or 5-membered intramolecular rings, which are essential for conformational stability. The presence of these intramolecular H-type close contacts has been clearly identified in the FTIR spectra, through the corresponding ν(OH) modes. Also, deviations to lower wavenumber of some of these hydroxyl stretching bands reflect the involvement of these groups in strong intermolecular interactions in the solid state. Additionally, the occurrence of these interactions affects the electronic delocalisation in this type of chromone derivatives, therefore determining their conformational preferences. The molecules with an (O^3H) group were predicted to be planar, as opposed to those having a (O^5H) moiety, which were deviated from planarity by about 15–20°.

For the catechol-containing systems, both hydroxylic groups from the catechol moiety always displayed the same orientation relative to the pyrone ring, due to a weak intramolecular interaction between the two adjacent hydroxylic groups. Although the DFT calculations predicted an anti conformation of these OH's relative to the carbonyl(s) as the most stable one, for FIS and QUER the vibrational band around 880 cm^{-1} was ascribed to syn conformations, while the feature at about 850 cm^{-1} was assigned to the anti orientation, thus reflecting the coexistence for both orientations in the solid state. Furthermore, in these molecules the C^7 hydroxyl seems to assume either an anti or a syn conformation in the solid state, which is evidenced by the large number of spectral features found for the (O^7H)–containing molecules.

Finally, FIS was studied in its hydrated form (often the commercial form of these compounds), and it should not be forgotten that the hydration water molecules are prone to interfere with both the inter- and intramolecular H-bond interactions, therefore leading to changes in the molecule's conformational preferences in the solid state. Hence, a study of the hydration process in these systems would certainty shed some light on their conformational behaviour, as well as on the consequent changes in the vibrational spectra. Moreover, vibrational studies on the temperature dependent phase behaviour in these compounds would allow to clarify the corresponding polymorphic equilibrium, and hopefully to detect and characterise the polymorphic species.

In sum, the present work highlights the close relationship between structure and activity for hydroxylated flavone derivatives, a thorough conformational analysis being essential for attaining a better understanding of their recognised antioxidant properties (which were evaluated in a parallel study [37]). Furthermore, this detailed knowledge of the conformational behaviour of this group of phytochemicals will allow a rational design of optimised chemopreventive agents of natural origin, with improved efficacy and safety.

Acknowledgments

The authors thank financial support from the Portuguese Foundation for Science and Technology – PEst-OE/QUI/UI0070/2011 and PhD grant SFRH/BD/40235/2007 (NFLM). The Chemistry Department of the University of Aveiro is acknowledged for use of the FT-Raman spectrometer.

Appendix A. Supplementary material

Supplementary data associated with this article can be found, in the online version, at http://dx.doi.org/10.1016/j.saa.2013.01.038.

References

[1] C. Kaur, H.C. Kapoor, Int. J. Food Sci. Technol. 36 (2001) 703.
[2] O. Blokhina, E. Virolainen, K.V. Fagerstedt, Ann. Bot. 91 (2003) 179.
[3] E. Riboli, T. Norat, Am. J. Clin. Nutr. 78 (2003) 559S.
[4] L. Bravo, Nutr. Rev. 56 (1998) 317.
[5] P.G. Pietta, J. Nat. Prod. 63 (2000) 1035.
[6] P. van't Veer, M.C. Jansen, M. Klerk, F.J. Kok, Public Health Nutr. 3 (2000) 103.
[7] C.G. Heijnen, G.R. Haenen, F.A. van Acker, W.J. van der Vijgh, A. Bast, Toxicol. In Vitro 15 (2001) 3.
[8] C.A. Gomes, T.G. da Cruz, J.L. Andrade, N. Milhazes, F. Borges, M.P. Marques, J. Med. Chem. 46 (2003) 5395.
[9] W. Ren, Z. Qiao, H. Wang, L. Zhu, L. Zhang, Med. Res. Rev. 23 (2003) 519.
[10] Y.J. Surh, Nat. Rev. Cancer 3 (2003) 768.
[11] T.J. Key, A. Schatzkin, W.C. Willett, N.E. Allen, E.A. Spencer, R.C. Travis, Public Health Nutr. 7 (2004) 187.
[12] B.A. Graf, P.E. Milbury, J.B. Blumberg, J. Med. Food 8 (2005) 281.
[13] P. Fresco, F. Borges, C. Diniz, M.P. Marques, Med. Res. Rev. 26 (2006) 747.
[14] B. Swinburn, Public Health Nutr. 12 (2009) 877.
[15] P. Fresco, F. Borges, M. Marques, C. Diniz, Curr. Pharm. Design 16 (2010) 114.
[16] G. Mandalari, R.M. Faulks, C. Bisignano, K.W. Waldron, A. Narbad, M.S. Wickham, FEMS Microbiol. Lett. 304 (2010) 116.
[17] C.J. Dillard, J.B. German, J. Sci. Food Agric. 80 (2000) 1744.
[18] E. Middleton Jr., C. Kandaswami, T.C. Theoharides, Pharmacol. Rev. 52 (2000) 673.
[19] B.H. Havsteen, Pharmacol. Ther. 96 (2002) 67.
[20] M.A. Soobrattee, V.S. Neergheen, A. Luximon-Ramma, O.I. Aruoma, T. Bahorun, Mutat. Res. – Fund. Mol. M 57 (9) (2005) 200.
[21] E. Haslam, Practical Polyphenolics: from Structure to Molecular Recognition and Physiological Action, Cambridge University Press, Cambridge, 1998.
[22] N.F. Machado, M.P. Marques, Curr. Bioact. Comp. 6 (2010) 76.
[23] H. Fang, W.D. Tong, L.M. Shi, R. Blair, R. Perkins, W. Branham, B.S. Hass, Q. Xie, S.L. Dial, C.L. Moland, D.M. Sheehan, Chem. Res. Toxicol. 14 (2001) 280.
[24] M. Recanatini, A. Bisi, A. Cavalli, F. Belluti, S. Gobbi, A. Rampa, P. Valenti, M. Palzer, A. Palusczak, R.W. Hartmann, J. Med. Chem. 44 (2001) 672.
[25] Y. Li, H. Fang, W. Xu, Y. Li, H. Fang, W. Xu, Mini Rev. Med. Chem. 7 (2007) 663.

[26] D. Bennardi, G. Romanelli, J. Jios, J. Autino, G. Baronetti, H. Thomas, Arkivoc xi (2008) 123.
[27] M. Grazul, E. Budzisz, Coordin. Chem. Rev. 253 (2009) 2588.
[28] K.N. Prasad, J. Hao, C. Yi, D. Zhang, S. Qiu, Y. Jiang, M. Zhang, F. Chen, J. Biomed. Biotechnol. 2009 (2009) 612805.
[29] M. Lopez-Lazaro, Mini Rev. Med. Chem. 9 (2009) 31.
[30] F. Casetti, W. Jung, U. Wölfle, J. Reuter, K. Neumann, B. Gilb, A. Wähling, S. Wagner, I. Merfort, C.M. Schempp, J. Photochem. Photobiol. B. Biol. 96 (2009) 260.
[31] G. Fraqueza, L.A.E. Batista de Carvalho, M.P.M. Marques, L. Maia, C.A. Ohlin, W.H. Casey, M. Aureliano, Dalton Trans. 41 (2012) 12749.
[32] M. Lopez-Lazaro, Curr. Med. Chem. – Anti-Cancer Agents 2 (2002) 691.
[33] K.E. Heim, A.R. Tagliaferro, D.J. Bobilya, J. Nutr. Biochem. 13 (2002) 572.
[34] D. Amic, D. Davidovic-Amic, D. Beslo, N. Trinajstic, Croat. Chem. Acta 76 (2003) 55.
[35] A. Seyoum, K. Asres, F.K. El-Fiky, Phytochem. 67 (2006) 2058.
[36] D. Prochazkova, I. Bousova, N. Wilhelmova, Fitoterapia 82 (2011) 513.
[37] M.M. Dias, N.F.L. Machado, M.P.M. Marques, Food Funct. 2 (2011) 595.
[38] M.J. Frisch, G.W. Trucks, H.B. Schlegel, G.E. Scuseria, M.A. Robb, J.R. Cheeseman, J.J.A. Montgomery, T. Vreven, K.N. Kudin, J.C. Burant, J.M.I. Millam, S.S.J. Tomasi, V. Barone, B. Mennucci, M. Cossi, G. Scalmani, N. Rega, G.A. Petersson, H. Nakatsuji, M. Hada, M. Ehara, K. Toyota, R. Fukuda, J. Hasegawa, M. Ishida, T. Nakajima, Y. Honda, O. Kitao, H. Nakai, M. Klene, X. Li, J.E. Knox, H.P. Hratchian, J.B. Cross, V. Bakken, C. Adamo, J. Jaramillo, R. Gomperts, R.E. Stratmann, O. Yazyev, A.J. Austin, R. Cammi, C. Pomelli, J.W. Ochterski, P.Y. Ayala, K. Morokuma, G.A. Voth, P. Salvador, J.J. Dannenberg, V.G. Zakrzewski, S. Dapprich, A.D. Daniels, M.C. Strain, O. Farkas, D.K. Malick, A.D. Rabuck, K. Raghavachari, J.B. Foresman, J.V. Ortiz, Q. Cui, A.G. Baboul, S. Clifford, J. Cioslowski, B.B. Stefanov, G. Liu, A. Liashenko, P. Piskorz, I. Komaromi, R.L. Martin, D.J. Fox, T. Keith, M.A. Al-Laham, C.Y. Peng, A. Nanayakkara, M. Challacombe, P.M.W. Gill, B. Johnson, W. Chen, M.W. Wong, J. Gonzalez, J.A. Pople, Gaussian 03, Revision D.01, Gaussian, Inc, Wallingford CT, 2004.
[39] C. Lee, W. Yang, R.G. Parr, Phys. Rev. B Condens. Matter 37 (1988) 785.
[40] B. Miehlich, A. Savin, H. Stoll, H. Preuss, Chem. Phys. Lett. 157 (1989) 200.
[41] A.D. Becke, Phys. Rev. A 38 (1988) 3098.
[42] A.D. Becke, J. Chem. Phys. 98 (1993) 1372.
[43] G.A. Petersson, A. Bennett, T.G. Tensfeldt, M.A. Allaham, W.A. Shirley, J. Mantzaris, J. Chem. Phys. 89 (1988) 2193.
[44] C. Peng, P.Y. Ayala, H.B. Schlegel, M.J. Frisch, J. Comput. Chem. 17 (1996) 49.
[45] J.P. Merrick, D. Moran, L. Radom, J. Phys. Chem. A 111 (2007) 11683.
[46] N.F.L. Machado, R. Valero, H.S. Domingos, J. Tomkinson, L.A.E. Batista de Carvalho, J.C. Otero, M.P.M. Marques, J. Vib. Spectrosc. 63 (2012) 325.
[47] J.M. Petroky, C. De Sá Valente, E.P. Kelson, S. Collins, J. Phys. Chem. A 106 (2002) 5.
[48] M.C. Etter, Z. Urbanczyklipkowska, S. Baer, P.F. Barbara, J. Mol. Struct. 144 (1986) 155.
[49] M. Shoja, Acta Crystallogr. Sect. C – Crystal Struct. Commun. 46 (1990) 517.
[50] G.Z. Jin, Y. Yamagata, K. Tomita, Acta Crystallogr. Sect. C – Cryst. Struct. Commun. 46 (1990) 310.
[51] C. Corredor, T. Teslova, M.V. Canamares, Z.G. Chen, J. Zhang, J.R. Lombardi, M. Leona, J. Vib. Spectrosc. 49 (2009) 190.
[52] Z. Jurasekova, G. Marconi, S. Sanchez-Cortes, A. Torreggiani, Biopolymers 91 (2009) 917.
[53] R. Sekine, J. Vongsvivut, E.G. Robertson, L. Spiccia, D. McNaughton, J. Phys. Chem. B 114 (2010) 7104.
[54] T. Teslova, C. Corredor, R. Livingstone, T. Spataru, R.L. Birke, J.R. Lombardi, M.V. Canamares, M. Leona, J. Raman Spectrosc. 38 (2007) 802.
[55] J.P. Cornard, L. Vrielynck, J.C. Merlin, J.C. Wallet, Spectrochim. Acta A 51 (1995) 913.
[56] R.D.H. Murray, P.H. Mccabe, Tetrahedron 25 (1969) 5819.
[57] R.D.H. Murray, P.H. Mccabe, T.C. Hogg, Tetrahedron 25 (1969) 5839.
[58] N. Sundaraganesan, G. Mariappan, S. Manoharan, Spectrochim. Acta A 87 (2012) 67.